Single-molecule FRET reveals sugar-induced conformational dynamics in LacY

Devdoot S. Majumdar[†], Irina Smirnova[‡], Vladimir Kasho[‡], Eyal Nir[§], Xiangxu Kong[§], Shimon Weiss[†‡§¶‖], and H. Ronald Kaback[†‡‖††]

[†]Molecular Biology Institute, Departments of [‡]Physiology, [§]Chemistry and Biochemistry, and [††]Microbiology, Immunology, and Molecular Genetics, and [¶]California NanoSystems Institute, University of California, Los Angeles, CA 90095-1662

Edited by Robert J. Silbey, Massachusetts Institute of Technology, Cambridge, MA, and approved April 4, 2007 (received for review February 1, 2007)

The N- and C-terminal six-helix bundles of lactose permease (LacY) form a large internal cavity open on the cytoplasmic side and closed on the periplasmic side with a single sugar-binding site at the apex of the cavity near the middle of the molecule. During sugar/H^+ symport, an outward-facing cavity is thought to open with closing of the inward-facing cavity so that the sugar-binding site is alternately accessible to either face of the membrane. In this communication, single-molecule fluorescence (Förster) resonance energy transfer is used to test this model with wild-type LacY and a conformationally restricted mutant. Pairs of Cys residues at the ends of two helices on the cytoplasmic or periplasmic sides of wild-type LacY and the mutant were labeled with appropriate donor and acceptor fluorophores, single-molecule fluorescence resonance energy transfer was determined in the absence and presence of sugar, and distance changes were calculated. With wild-type LacY, binding of a galactopyranoside, but not a glucopyranoside, results in a decrease in distance on the cytoplasmic side and an increase in distance on the periplasmic side. In contrast, with the mutant, a more pronounced decrease in distance and in distance distribution is observed on the cytoplasmic side, but there is no change on the periplasmic side. The results are consistent with the alternating access model and indicate that the defect in the mutant is due to impaired ligand-induced flexibility on the periplasmic side.

lactose permease | major facilitator superfamily | single-molecule spectroscopy | transporters

The lactose permease of *Escherichia coli* (LacY), a member of the major facilitator superfamily, utilizes free energy stored in an electrochemical H^+ gradient ($\Delta\mu_{H+}$) to drive active transport by coupling the downhill, stoichiometric translocation of H^+ with $\Delta\mu_{H+}$ to the uphill accumulation of galactopyranosides. Conversely, in the absence of $\Delta\mu_{H+}$, LacY utilizes free energy released from downhill translocation of galactosides in either direction to drive uphill translocation of H^+ with generation of $\Delta\mu_{H+}$ (reviewed in ref. 1).

An x-ray structure of mutant C154G, which binds ligand as well as wild-type LacY but catalyzes very little transport and is compromised conformationally (2–5), has been solved in an inward-facing conformation with bound ligand (6, 7). Notably, wild-type LacY has the same global fold (1, 8). The symporter contains 12 transmembrane α-helices organized in two pseudosymmetrical bundles. The N- and C-terminal six-helix bundles form a large internal cavity open to the cytoplasm, and a single sugar-binding site is present at the apex of the cavity near the approximate middle of the molecule.

When compared with the x-ray structure, distances approximated from cross-linking of paired Cys residues across the inward-facing cavity are underestimated, and there is no access to the sugar-binding site from the external surface (6). Therefore, it was suggested that during transport the inward-facing cavity closes with opening of an outward-facing cavity so that the sugar-binding site is alternately accessible to either face of the membrane, and a similar model was proposed for the glycerol phosphate/phosphate antiporter GlpT (9), a related protein. Recent findings (10) from site-directed alkylation of Cys residues at almost every position in LacY support the alternating access model.

Table 1. Properties of cysteine LacY mutants double labeled by Alexa 488 and Alexa 647 fluorophores

LacY mutant	Extent of labeling,[†] mol per mol of protein		NPG binding,[‡] % of binding to nonlabeled mutant
	A488	A647	
R73C/S401C/WT	0.6	0.6	98
R73C/S401C/C154G	0.7	0.8	93
I164C/S375C/WT	1	0.7	79
I164C/S375C/C154G	0.8	0.8	93

[†]Estimated from absorption spectra (see *Materials and Methods*).
[‡]Detected by direct sugar-binding assay based on Trp-NPG FRET as described in *Materials and Methods* (32).

The heat of ligand binding to wild-type LacY and the C154G mutant has been measured (11). The affinity of wild-type or mutant LacY for ligand and the change in free energy (ΔG) upon binding are similar. However, in the wild type, ΔG is due primarily to an increase in entropy, whereas in marked contrast, an increase in enthalpy is responsible for ΔG in the mutant. Thus, wild-type LacY behaves as if there are multiple ligand-bound conformational states, whereas the mutant is severely restricted.

Single-molecule fluorescence (Förster) resonance energy transfer (sm-FRET) (12–14) has been applied to the study of relatively few membrane proteins [e.g., F_1F_o-ATP synthase (15), epidermal growth factor (16), the antiporter OxlT (17), and SNARE proteins (18, 19)]. Structural dynamics in these proteins has been probed by measuring sm-FRET either from freely diffusing molecules or by recording a time-trajectory from a single, immobilized protein.

Here, we use sm-FRET by alternating laser excitation spectroscopy (20–23) to study ligand-induced distance changes on the cytoplasmic and periplasmic sides of the membrane protein LacY, freely diffusing in detergent micelles. The results provide

Author contributions: S.W. and H.R.K. designed research; D.S.M., I.S., V.K., and X.K. performed research; I.S. and V.K. contributed new reagents/analytic tools; D.S.M., I.S., V.K., and E.N. analyzed data; and D.S.M., I.S., V.K., E.N., S.W., and H.R.K. wrote the paper.

The authors declare no conflict of interest.

This article is a PNAS Direct Submission.

Abbreviations: NPG, 4-nitrophenyl-α-D-galactopyranoside; NPGlc, 4-nitrophenyl-α-D-glucopyranoside; sm-FRET, single-molecule fluorescence (Förster) resonance energy transfer.

‖To whom correspondence may be addressed. E-mail: sweiss@chem.ucla.edu or rkaback@mednet.ucla.edu.

This article contains supporting information online at www.pnas.org/cgi/content/full/0700969104/DC1.

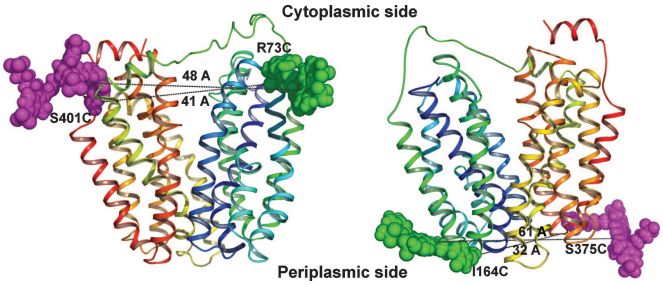

Fig. 1. Structural modeling of LacY double-labeled with Alexa fluorophores at Cys pairs introduced at the cytoplasmic ends of helices III and XII (R73C/S401C) (*Left*) or the periplasmic ends of helices V and XI (I164C/R375C) (*Right*). Backbone of LacY rendered as ribbons rainbow colored from blue (helix 1) to red (helix 12) with hydrophilic cavity open to cytoplasmic side. Attached fluorophores colored in green (Alexa 488) or magenta (Alexa 647) and shown in space-filling representation. Estimated distances between C_α atoms of the Cys pairs and between centers of the fluorophores are 41 and 48 Å (cytoplasmic), and 32 and 61 Å (periplasmic), respectively.

further support for the alternating access model in wild-type LacY and suggest that although the cytoplasmic cavity also narrows in the C154G mutant, the periplasmic side remains fixed in the presence of ligand. The results are also consistent with the conclusion (11) that sugar binding induces primarily an entropic change in wild-type LacY, in marked contrast to mutant C154G, which exhibits an enthalpic change.

Results

Mutants. Cysteine pairs were introduced into wild-type and C154G LacY. None of the native Cys residues in LacY react with maleimides under near stoichiometric conditions except for Cys-148, which is readily protected by substrate (24). Two mutant pairs [R73C/S401C (helices III and XII) on the cytoplasmic side and I164C/S375C (helices V and XI) on the periplasmic side] satisfy the following requirements: (*i*) both positions are at the ends of transmembrane helices, (*ii*) individual Cys replacements have little or no effect on lactose transport (25–28), (*iii*) Cys residues at each of the four positions react with the maleimide-based Alexa dyes (Table 1), (*iv*) double-Cys mutants labeled with fluorophores bind sugar effectively (Table 1), and (*v*) distances between bound fluorophores in both double-Cys mutants are within R_0 (Förster radius) for the Alexa dyes used (≈50 Å).

Because the size of both Alexa moieties is significant, the interdye distance depends on the relative orientation of the dyes as determined by the mobility of the fluorophores and the structural flexibility of LacY. Structural modeling [see supporting information (SI) *Materials and Methods*] predicts different orientations of the donor (D)–acceptor (A) pairs on either side of the protein; these positions are likely to be relatively rigid due to placement in α-helices (Fig. 1). Approximate distances between D and A moieties are 48 Å for the cytoplasmic pair or 61 Å for periplasmic pair; distances that fall well within the linear range of the sm-FRET "ruler," as they are near R_0 of both Alexa dyes (see *Materials and Methods*).

Each of the four double-labeled samples displays significant FRET. However, mutants labeled with D only or A only and then mixed exhibit no FRET whatsoever. Thus, there is little or no aggregation. It is also notable that changes in FRET are not observed in the presence of galactopyranosides when ensemble measurements are carried out with a conventional fluorimeter (data not shown).

Structural Changes at the Cytoplasmic Side. sm-FRET is determined from bursts of fluorescence detected during diffusion of labeled molecules through a focused laser beam using alternating laser excitation spectroscopy (21). Bursts are recognized by a dual-channel burst search, which identifies bursts containing both D and A (29). For each burst, the apparent energy transfer efficiency (or proximity ratio, E^*) and the stoichiometry (S) are calculated and binned into a two-dimensional (2D) S–E^* histogram (Figs. 2*A* and 4*A*). D- and A-only populations are filtered out, and E^* values of the D-A species are projected onto a one-dimensional (1D) FRET histogram (Figs. 2 *B* and *C*, 3*A*, and 4 *B* and *C*).

Each sample was monitored for changes in E^* in response to a relatively high-affinity ligand, 4-nitrophenyl-α-D-galactopyranoside (NPG), or the analogue, 4-nitrophenyl-α-D-glucopyranoside (NPGlc), which exhibits no detectable binding (30–32). R73C/S401C LacY double-labeled on the cytoplasmic side (helices III and XII) exhibits an E^* distribution with mean $\langle E^* \rangle = 0.536 \pm 0.013$ [Fig. 2 *A1* and *B* (gray area)]. Addition of NPG results in a small but reproducible shift to $\langle E^* \rangle = 0.584 \pm 0.009$ [Fig. 2*B* (red line)], consistent with a small but reproducible decrease in distance. No

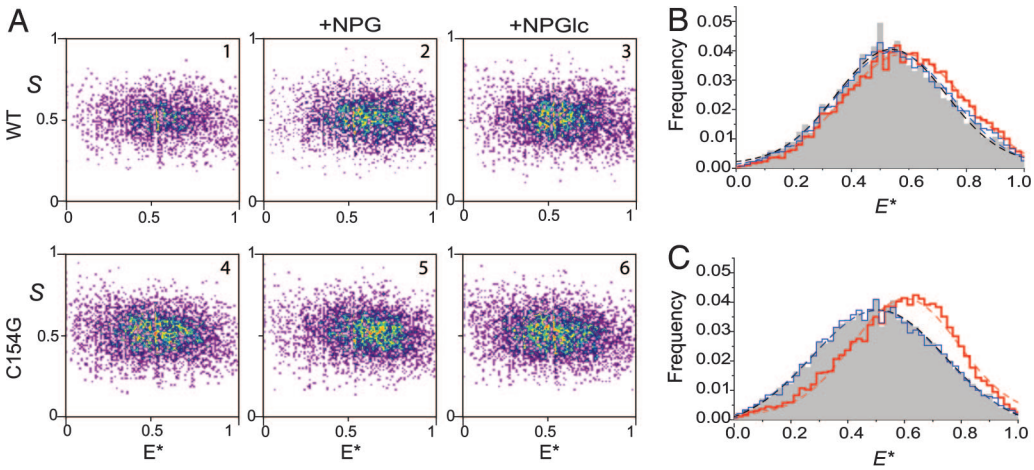

Fig. 2. Ligand-induced effects on the FRET distribution E^* at the cytoplasmic side of LacY (R73C/S401C, helices III and XII). (*A*) Two-dimensional S–E^* histograms corresponding to wild-type (*A1–A3*) and C154G mutant (*A4–A6*) LacY. Measurements for each construct were obtained in the absence of sugar (*A1* and *A4*) and in the presence of 1 mM (saturating) NPG (*A2* and *A5*) or 1 mM NPGlc (*A3* and *A6*). (*B* and *C*) Comparison of sugar effects on normalized E^* histograms from *A* for wild-type LacY (*B*) and C154G LacY (*C*). Gray bins, no sugar added; red line, 1 mM NPG; blue line, 1 mM NPGlc; broken lines, Gaussian fits to the data with the corrected E values given in Table 2.

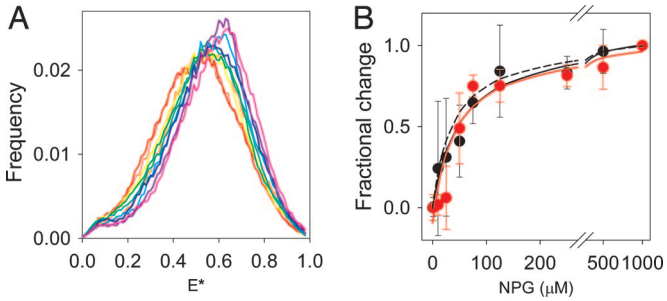

Fig. 3. Concentration dependence of ligand-induced effects on $\langle E^* \rangle$ and ΔE^* at the cytoplasmic side of LacY (R73C/S401C/C154G, helices III and XII). (*A*) E^* distribution without added sugar (red) and with nine NPG concentrations increasing from 1 μM (orange) to 1,000 μM (purple). (*B*) Fractional change of the fitted Gaussian parameters of histograms from *A* plotted as a function of NPG concentration. Red, relative $\langle E^* \rangle$ shift; black, relative ΔE^* change. The maximum change in $\langle E^* \rangle$ and ΔE^* at saturating concentration of NPG (1 mM) corresponds to 1. Solid lines, hyperbolic fit to each data set; broken line, theoretical curve showing NPG binding to LacY with K_d of 38 μM as measured by stopped-flow (32).

effect of NPGlc ($\langle E^* \rangle = 0.547 \pm 0.001$) is observed [Fig. 2*B* (blue line)]. In contrast, mutant C154G, which is conformationally restricted (4, 5, 11) and labeled at the same positions, exhibits $\langle E^* \rangle = 0.512 \pm 0.007$ [Fig. 2 *A4* and *C* (gray area)], suggesting a slight increase in distance relative to the wild-type (compare gray areas in Fig. 2 *B* and *C*). More dramatically, addition of NPG results in a significant shift, $\langle E^* \rangle = 0.611 \pm 0.007$, indicating a reduction in distance between D and A [Fig. 2*C* (red line)]. Because addition of NPGlc has no effect whatsoever [Fig. 2*C* (blue line)], it is concluded that the changes in the E^* distribution are specific to the galactopyranoside ring.

To test further the binding specificity of NPG to the double-labeled R73C/S401C/C154G LacY mutant, E^* histograms were recorded as a function of NPG concentration (Fig. 3*A*). The relative changes (see definition in *SI Materials and Methods*) in the average E^* ($\langle E^* \rangle$) and in the average width of the distribution ($\langle \Delta E^* \rangle$) are plotted as a function of NPG concentration in Fig. 3*B*. Increasing NPG concentration is accompanied by a shift in $\langle E^* \rangle$ to higher values with a concomitant decrease in $\langle \Delta E^* \rangle$. Apparent K_D values extracted from the $\langle E^* \rangle$ and $\langle \Delta E^* \rangle$ titration curves are 40 $\pm$ 14 and 52 $\pm$ 14 μM, respectively. These values are in good agreement with those obtained by using other methods (4, 32).

Each cysteine position described herein was labeled individually with D and A on both wild-type and C154G backgrounds. The quantum yield of D-labeled molecules and spectral overlap of D and A was used to calculate R_0 for each construct. Furthermore, because conversion from E^* to E relies on an approximation to obtain the γ-correction factor (see *SI Materials and Methods*), we achieve approximate E values and corresponding interdye distances. On the cytoplasmic side, the average distances between dyes are calculated to be ≈51.3 Å for wild-type and ≈52.9 Å for C154G LacY without bound sugar (Table 2), which are in general agreement with modeling (Fig. 1). NPG binding to wild-type LacY is associated with a small decrease in distance (≈1.6 Å), whereas the C154G mutant exhibits a larger decrease of ≈3.4 Å and a narrowing of $\langle \Delta E^* \rangle$ (Fig. 3).

Structural Changes at the Periplasmic Side. Analysis of E^* distribution for I164C/R375C LacY double-labeled on the periplasmic side (helices V and XI) exhibits $\langle E^* \rangle = 0.416 \pm 0.004$ [Fig. 4 *A1* and *B* (gray area)]. Addition of NPG results in a shift to $\langle E^* \rangle = 0.344 \pm 0.004$, indicating an increase in the distance between the dyes upon ligand binding [Fig. 4*B* (red line)]. NPGlc addition results in no significant change in the E^* distribution [Fig. 4*B* (blue line)]. C154G

Table 2. Effect of sugar binding on sm-FRET parameters

Location of double-labeled Cys pairs	LacY	No sugar			NPG (1 mM)			NPGlc (1 mM)			NPG-induced distance change, Å
		E^*	$E^\dagger$	Distance, Å‡	E^*	E	Distance, Å	E^*	E	Distance, Å	
Cytoplasmic side 73/401	Wildtype	0.536 (±0.013)	0.468 (±0.013)	51.5	0.584 (±0.009)	0.523 (±0.009)	49.7	0.547 (±0.001)	0.480 (±0.001)	51.1	1.4–1.8 decrease
	154G	0.512 (±0.007)	0.444 (±0.008)	53.1	0.611 (±0.007)	0.552 (±0.009)	49.5	0.523 (±0.026)	0.456 (±0.030)	52.7	3.2–3.6 decrease
Periplasmic side 164/375	Wildtype	0.416 (±0.004)	0.342 (±0.003)	56.8	0.344 (±0.004)	0.264 (±0.004)	60.4	0.411 (±0.010)	0.336 (±0.011)	57.0	3.4–3.6 increase
	154G	0.360 (±0.001)	0.282 (±0.001)	57.8	0.363 (±0.010)	0.283 (±0.008)	57.8	0.359 (±0.001)	0.279 (±0.002)	57.9	No significant change

†E is a corrected sm-FRET efficiency (23).
‡Distances have a precision of ±1 Å.

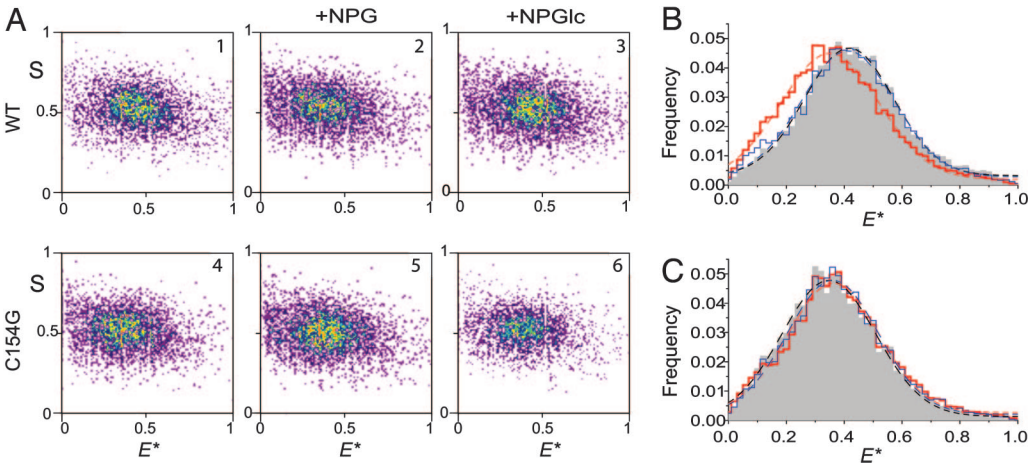

Fig. 4. Ligand-induced effects on the FRET distribution E^* at the periplasmic side of LacY (I164C/S375C, helices V and XI). All details are as described in Fig. 2.

LacY labeled at the same positions exhibits $\langle E^* \rangle = 0.360 \pm 0.001$, and addition of NPG or NPGlc does not produce a significant change (Fig. 4*C*).

The average distances between dyes are calculated to be ≈56.9 Å for wild-type and ≈57.8 Å for C154G LacY without bound sugar (Table 2) based on determined R_0. NPG binding to wild type is associated with an increase in distance (≈3.5 Å) and a slight increase in $\langle \Delta E^* \rangle$, whereas the C154G mutant exhibits no significant change.

Discussion

sm-FRET is used here to investigate the effects of sugar binding on local distance and distance distribution changes between the cytoplasmic ends of helices III and XII or the periplasmic ends of helices V and XI in wild-type LacY and the conformationally restricted mutant C154G. The measured interdye distances calculated from sm-FRET are comparable to those predicted from modeling (compare Fig. 1 with Table 2). Whereas sugar binding in the wild-type background appears to decrease distance (i.e., increased $\langle E^* \rangle$) between the cytoplasmic ends of helices III and XII, the effect is significantly more pronounced in the mutant background and is also accompanied by a reduction in $\langle \Delta E^* \rangle$. In marked contrast, the periplasmic ends of helices V and XI appear to move apart (i.e., decreased $\langle E^* \rangle$) as a result of sugar binding in the wild type, but no change whatsoever is detected with the C154G mutant (Table 2).

Analysis of the shape of the E^* histogram provides information about static distance changes, as well as changes in the distribution of conformers and interconversion rates between them (29). The shape of the E^* histogram of a single conformer (a single E^* value) is determined by shot noise. Multiple conformers (multiple E^* values) result in broadening or splitting of the E^* histogram. If each conformer is long-lived (longer than the transit time through the confocal volume), the resulting histogram will be a superposition of the individual shot-noise broadened states. If the interconversion between conformers is faster than the transit time, the E^* distribution averages out to a single E^* value (broadened by shot noise). When interconversion between conformers is on the order of the transit time, the resulting histogram width depends on the rates.

Both wild-type and C154G LacY without and with ligand, exhibit conformational heterogeneity on the cytoplasmic and periplasmic sides [distributions are wide and not limited by shot noise (see SI Fig. 6)]. The distance and distance distribution changes may be due to interconversion between two states (minimally) at rates that are ≈10 times slower than diffusion [interconversion rates faster than diffusion would result in narrower peaks; slower rates do not fit the data (see SI Fig. 7)]. An alternative possibility is that the wild type and the mutant have multiple static conformers in the unliganded state, and upon binding, the number of conformers is reduced for the mutant and increased for the wild type. For a detailed discussion, see *SI Materials and Methods*.

The sm-FRET findings with wild-type LacY are consistent with extensive site-directed alkylation studies (10) that support an alternating access model for galactoside/H^+ symport (1, 6). By this means, the single sugar-binding site in LacY in the approximate middle of the molecule is alternately exposed to either side of the membrane due to opening and closing of cytoplasmic and periplasmic hydrophilic cavities. In this regard, it is particularly noteworthy that the cytoplasmic ends of helices III and XII in the C154G mutant apparently move closer upon sugar binding, whereas the periplasmic ends of helices V and XI exhibit no change. The observations suggest that the C154G mutation may markedly decrease the ability of LacY to change conformation on the periplasmic side (2–5).

The crystal structure of wild-type LacY exhibits an inward-facing conformation much like the C154G mutant (1, 8). Furthermore, ligand binding markedly increases the apparent ac-

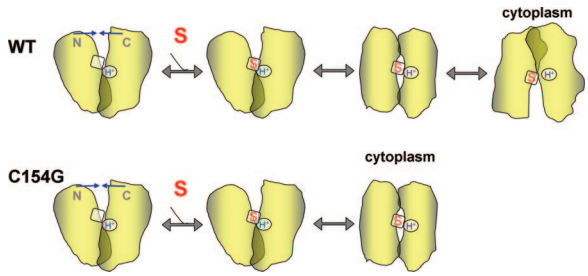

Fig. 5. Cartoon model illustrating global conformational changes detected by sm-FRET upon sugar binding to wild-type LacY and C154G mutant. Without bound sugar (left) protein is in the protonated state with an inward-facing hydrophilic cavity. Without ligand, both molecules have multiple conformations on the cytoplasmic side (arrows). This conformation is the most energetically stable among multiple unliganded conformers. Binding of sugar induces a global conformational change in both wild-type LacY and C154G mutant resulting in closing of the inward-facing hydrophilic cavity. A cavity opens on the periplasmic in wild-type LacY allowing substrate to be released, and conformational heterogeneity increases after sugar binding. In contrast, the periplasmic cavity in C154G mutant does not form easily after sugar binding, corresponding to a reduced number of conformers in the ligand-bound state and restricted access for the sugar from periplasmic side.

cessibility/reactivity of a number of engineered Cys residues on the periplasmic side of the protein with a distribution, suggesting that sugar binding opens a hydrophilic pathway on the periplasmic side of the molecule. Thus, it seems reasonable to conclude that the crystal structure of LacY is similar to that in the membrane—the inward-facing conformation. If this is so, the time of occupancy in the outward-facing conformation is likely to be relatively short because the inward-facing conformation probably represents the lowest free-energy state.

Taken together, isothermal scanning calorimetry studies (11), site-directed alkylation studies (10), and the sm-FRET studies presented here (carried out on only two pairs of helices thus far) are consistent with a picture in which ligand binding leads primarily to an entropic change in the wild type and an enthalpic change in the C154G mutant. Thus, wild-type LacY behaves as if there are multiple ligand-bound conformational states, whereas the mutant is severely restricted because of an inability to move on the periplasmic side. Moreover, the findings are consistent with the notion that cytoplasmic and periplasmic movements of the helices in LacY are not necessarily coordinated, a consideration that may be related to the irregular nature of many of the helices. It follows that the N- and C-terminal helical bundles in LacY probably do not move as rigid bodies.

Fig. 5 proposes a simple cartoon model for the conclusions.

Materials and Methods

Fluorophores. Alexa 488 C_5-maleimide and Alexa 647 C_2-maleimide fluorophores were purchased from Molecular Probes (Invitrogen).

Labeling of LacY mutants with Alexa Dyes. Mutants with a single additional Cys residue (40–50 μM) were incubated with equimolar concentrations of either Alexa Fluor 488 C_5-maleimide or Alexa Fluor 647 C_2-maleimide in 50 mM NaP_i buffer (pH 7.0), with 0.02% dodecyl-β-D-maltopyranoside in the presence of 15 mM TDG added for protection of Cys-148 against alkylation. The reaction was carried out for 30 min at room temperature in the dark. Double-Cys mutants were labeled in the same buffer sequentially: first, an equimolar concentration of Alexa Fluor 647 C_2-maleimide was added for 30 min in the dark, then Alexa Fluor 488 C_5-maleimide was added and the reaction was carried out for another 45 min. TDG and unreacted fluorophores were removed by buffer exchange on an Amicon Ultra-15 concentrator with a cut-off of 30 kDa (Millipore). The extent of the labeling was estimated from absorption spectra of labeled mutants by measuring peak maxima at 280, 488, and 647 nm for protein and fluorophores, respectively, using a Hitachi model 24 UV-vis scanning spectrophotometer. Control experiments with labeling under the same conditions of either wild-type or C154G LacY that lack introduced Cys pairs resulted in no significant incorporation of Alexa dyes. Final samples (0.5 mg/ml) were frozen in liquid nitrogen and stored at −80°C before use.

Binding Assays. Sugar binding to purified LacY mutants was measured before and after labeling with Alexa fluorophores by using a direct sugar-binding assay based on Trp-151-NPG FRET as described in ref. 32. Trp emission spectra (excitation 295 nm) of LacY mutants (0.4 μM) in 50 mM NaP_i (pH 7.5)/0.02% dodecyl-β-D-maltopyranoside were recorded first in the presence of 100 μM NPG, and then after the addition of 10 mM TDG used for displacement of bound NPG. The relative Trp fluorescence increase after TDG addition quantified the level of specific sugar binding. Spectral properties of used Alexa fluorophores do not interfere with Trp-NPG FRET. The ability of LacY mutants modified with Alexa fluorophores to bind NPG was 70–100% of that for LacY before modification.

Sample Preparation. For measurement, LacY was diluted to 200 pM in 50 mM sodium phosphate (pH 7.5), 0.02% dodecyl-β-D-maltopyranoside, and 100 μg/ml BSA, with or without sugar. An observation chamber for a 5-μl drop was constructed by using an 8-mm hole in a 0.5-mm-thick silicone gasket between two no. 1 coverslips.

Microscope Setup, Data Collection, and Analysis. Measurements were made by using an oil-immersion objective (Zeiss; ×100, 1.4 N.A.) inverted fluorescence microscope, described elsewhere. Molecules were excited by alternating laser excitation (21) at 470 and 640 nm (TOPTICA Photonics iPulse and iBeam, respectively) with an alternation period of 100 μs and a duty cycle of 50%. Excitation intensities were 50–60 μW for 470 nm and 10 μW for 640 nm. The beam was focused by an oil-immersion objective. Fluorescence was collected through the same objective and refocused onto a 100-μm pinhole to reject out-of-focus light. The collected photons were split by a dichroic mirror (630DRLP; Omega Optical), filtered (520-DF-40, 660-LP), and detected by avalanche photodiodes (SPCM-AQR-14; PerkinElmer). Time of arrival of each detected photon was stored on a computer for future analysis (29). Data were typically collected for 10–15 min, yielding ≈3,000 bursts. Each experiment was repeated three to five times. Results (and their errors) were calculated from these data sets. Detailed descriptions of data analysis and fitting protocols are given in *SI Materials and Methods*.

All other materials, construction of mutants, purification of proteins, ensemble fluorescence measurements, molecular modeling, and sm-FRET data analysis are described in *SI Materials and Methods*.

We thank M. Jäger, L. Guan, and Y. Korlann for helpful scientific discussions and J. Sugihara for excellent technical assistance. This work was supported in part by National Institutes of Health Grants DK51131, DK069463, and GM074929; National Science Foundation Grant 0450970 (to H.R.K.); National Science Foundation Frontiers in Integrative Biological Research Grant 0623664 (to S.W.); Department of Energy Grant DE-FG02-04ER63938 (to S.W.); and the Center for Biophotonics, a National Science Foundation Science and Technology Center, managed by the University of California, Davis, under Cooperative Agreement PHY0120999. E.N. is supported by the Human Frontier Science Program.

1. Guan L, Kaback HR (2006) *Annu Rev Biophys Biomol Struct* 35:67–91.
2. Menick DR, Sarkar HK, Poonian MS, Kaback HR (1985) *Biochem Biophys Res Commun* 132:162–170.
3. van Iwaarden PR, Driessen AJ, Lolkema JS, Kaback HR, Konings WN (1993) *Biochemistry* 32:5419–5424.
4. Smirnova IN, Kaback HR (2003) *Biochemistry* 42:3025–3031.
5. Ermolova NV, Smirnova IN, Kasho VN, Kaback HR (2005) *Biochemistry* 44:7669–7677.
6. Abramson J, Smirnova I, Kasho V, Verner G, Kaback HR, Iwata S (2003) *Science* 301:610–615.
7. Mirza O, Guan L, Verner G, Iwata S, Kaback HR (2006) *EMBO J* 25:1177–1183.
8. Guan L, Smirnova IN, Verner G, Nagamoni S, Kaback HR (2006) *Proc Natl Acad Sci USA* 103:1723–1726.
9. Huang Y, Lemieux MJ, Song J, Auer M, Wang DN (2003) *Science* 301:616–620.
10. Kaback HR, Dunten R, Frillingos S, Venkatesan P, Kwaw I, Zhang W, Ermolova N (2007) *Proc Natl Acad Sci USA* 104:491–494.
11. Nie Y, Smirnova I, Kasho V, Kaback, HR (2006) 281:35779–35784.
12. Deniz AA, Laurence TA, Beligere GS, Dahan M, Martin AB, Chemla DS, Dawson PE, Schultz PG, Weiss S (2000) *Proc Natl Acad Sci USA* 97:5179–5184.
13. Ha T, Enderle T, Ogletree DF, Chemla DS, Selvin PR, Weiss S (1996) *Proc Natl Acad Sci USA* 93:6264–6268.
14. Weiss S (1999) *Science* 283:1676–1683.
15. Diez M, Zimmermann B, Borsch M, Konig M, Schweinberger E, Steigmiller S, Reuter R, Felekyan S, Kudryavtsev V, Seidel CA, Graber P (2004) *Nat Struct Mol Biol* 11:135–141.
16. Sako Y, Minoghchi S, Yanagida T (2000) *Nat Cell Biol* 2:168–172.

17. Lesoine JF, Holmberg B, Maloney P, Wang X, Novotny L, Knauf PA (2006) *Acta Physiol* 187:141–147.
18. Margittai M, Widengren J, Schweinberger E, Schroder GF, Felekyan S, Haustein E, Konig M, Fasshauer D, Grubmuller H, Jahn R, Seidel CA (2003) *Proc Natl Acad Sci USA* 100:15516–15521.
19. Weninger K, Bowen ME, Chu S, Brunger AT (2003) *Proc Natl Acad Sci USA* 100:14800–14805.
20. Kapanidis AN, Laurence TA, Lee NK, Margeat E, Kong X, Weiss S (2005) *Acc Chem Res* 38:523–533.
21. Kapanidis AN, Lee NK, Laurence TA, Doose S, Margeat E, Weiss S (2004) *Proc Natl Acad Sci USA* 101:8936–8941.
22. Kapanidis AN, Margeat E, Ho SO, Kortkhonjia E, Weiss S, Ebright RH (2006) *Science* 314:1144–1147.
23. Lee NK, Kapanidis AN, Wang Y, Michalet X, Mukhopadhyay J, Ebright RH, Weiss S (2005) *Biophys J* 88:2939–2953.
24. le Coutre J, Whitelegge JP, Gross A, Turk E, Wright EM, Kaback HR, Faull KF (2000) *Biochemistry* 39:4237–4242.
25. Sahin-Tóth M, Frillingos S, Bibi E, Gonzalez A, Kaback HR (1994) *Protein Sci* 3:2302–2310.
26. Frillingos S, Kaback HR (1996) *Biochemistry* 35:5333–5338.
27. He MM, Sun J, Kaback HR (1996) *Biochemistry* 35:12909–12914.
28. Frillingos S, Sahin-Toth M, Wu J, Kaback HR (1998) *FASEB J* 12:1281–1299.
29. Nir E, Michalet X, Hamadani KM, Laurence TA, Neuhauser D, Kovchegov Y, Weiss S (2006) *J Phys Chem B* 110:22103–22124.
30. Rudnick G, Schuldiner S, Kaback HR (1976) *Biochemistry* 15:5126–5131.
31. Sahin-Tóth M, Gunawan P, Lawrence MC, Toyokuni T, Kaback HR (2002) *Biochemistry* 41:13039–13045.
32. Smirnova IN, Kasho VN, Kaback HR (2006) *Biochemistry* 45:15279–15287.